Lattice dynamics of a mixed diatomic lattice

S. C. Varshney* and J. F. Vetelino
Department of Electrical Engineering, University of Maine, Orono, Maine 04473

S. S. Mitra
Department of Electrical Engineering, University of Rhode Island, Kingston, Rhode Island 02881

I. F. Chang
IBM Thomas J. Watson Research Center, Yorktown Heights, New York 10598

(Received 24 October 1974; revised manuscript received 2 June 1975)

A pseudo-unit-cell model is utilized to calculate some lattice-dynamical properties of a mixed diatomic lattice of the form $AB_{1-x}C_x$, where $0 \leq x \leq 1$. The pseudo unit cell is formed by A, $(1-x)B$, and xC ions and the resulting mixed crystal lattice is a repetition of such cells. The lattice dynamics of both a linear and a three-dimensional mixed zinc-blende lattice have been studied. The lattice-dynamical model consists of central and noncentral short- and long-range interactions among ions of appropriate effective ionic charge. The model parameters are deduced from physical observables such as the elastic constants and the long-wavelength optical and impurity mode frequencies of the end systems when $x \to 0$ and $x \to 1$. Explicit calculations for the phonon dispersion and frequency distribution function have been performed for the linear mixed diatomic lattice and for $ZnS_{1-x}Se_x$ and $GaP_{1-x}As_x$.

I. INTRODUCTION

The study of mixed crystals can be dated back to as early as 1928.[1] The early work[2-4] on the lattice dynamics of disordered crystal systems was in most cases of a formal mathematical nature and therefore not easily adaptable for computational purposes. Several phenomenological models[5-10] have been proposed to study the vibrations of mixed-crystal systems. Verleur and Barker[7] considered a cluster model to account for the two-mode behavior of the mixed crystals $GaP_{1-x}As_x$ and $CdS_{1-x}Se_x$. This model assumed that like negative ions clustered around positive ions or vice versa depending on whether the impurity was an anion or a cation. In the random-element-isodisplacement (REI) model, Chen, Shockley, and Pearson[8] assumed that in a mixed crystal $AB_{1-x}C_x$, the B and C atoms are distributed on the anion sublattice and the anions of like species vibrate in phase with identical amplitudes against the cations which also vibrate as a rigid unit. Later, Chang and Mitra[9] modified the REI model to include the polarization field. Subsequently, Chang and Mitra[10] proposed the pseudo-unit-cell model and predicted the zone-boundary phonons of systems exhibiting the two-mode behavior at the zone center. Recently, there has been interest in using the Green's-function technique[11] and the coherent-potential-approximation technique[12-14] to study the lattice dynamics of mixed crystals. A review of the various types of mixed crystal models and relevant experimental data is given by Chang and Mitra.[10] At present, complete calculations for the phonon frequencies in an actual three-dimensional crystal have not been performed.

A natural "brute force" technique to calculate the phonon frequencies of a lattice is to start with a large finite lattice and then permute the various number of ways to configuratively orient the lattice depending upon the concentration x. For each possible configuration, the phonon frequencies would be calculated and the resulting ensemble would then be averaged to obtain a representation of the phonon frequencies in the mixed lattice. This technique would, however, be very tedious and long owing to the number of configurational orientations, and the violation of lattice periodicity in most of the configurations. For values of x approaching either zero or unity, the Green's-function technique could be applied. However, as the impurity concentration increases, the impurity-impurity interactions become significant. This causes the Green's-function approach to become very complicated.

The purpose of this paper is to calculate the phonon dispersion and the frequency distribution function based on a probabilistic repetitive unit cell defined as a pseudo unit cell.[10] Calculations have been performed for both a mixed linear diatomic chain and a mixed three-dimensional zinc-blende lattice. The pseudo unit cell is formed by the ions A, $(1-x)B$, and xC. Although this unit cell is simple it is obviously unphysical as far as the exact representation of the lattice. The fact that it obeys translational symmetry is a physical drawback. In spite of these deficiencies, however, this model has proven[7-10] to be a simple approach by which one can estimate general features of the

optical properties of mixed diatomic crystals. In particular, this model has theoretically verified[10] the experimental behavior of certain zone-center and zone-boundary phonons in mixed diatomic crystals. In view of the simplicity and previous success of this model, it was decided to extend the calculations to all wave vectors to see if the model has merit in mixed-crystal lattice-dynamical calculations. In the linear-chain lattice and the mixed zinc-blende lattice, the modified rigid-ion (MRI) model[15] is used to predict the lattice dynamics. The MRI model consists of short-range central and noncentral repulsive interactions and long-range Coulomb interactions among ions of appropriate effective ionic charge. The model parameters of the mixed crystal of the form $AB_{1-x}C_x$ are deduced from the elastic constants, optical-mode frequencies, and impurity-mode frequencies of the host crystals. The model parameters along with the lattice constant are assumed to vary linearly as a function of concentration. Explicit calculations have been performed for a hypothetical mixed linear chain and for $ZnS_{1-x}Se_x$ and $GaP_{1-x}As_x$. The phonon dispersion in various symmetry directions and the frequency distribution function are obtained as a function of concentration.

II. MIXED LINEAR DIATOMIC CHAIN

A. Pseudo unit cell

The unit cell as defined in perfect crystals cannot be uniquely defined for the mixed crystals. However, the mixed-crystal problem may be treated in a manner similar to the pure crystal case, if certain assumptions are made on the distribution of the ions in the lattice. In a mixed crystal, $AB_{1-x}C_x$ where $0 \leq x \leq 1$, the B and C ions are assumed to be distributed randomly in their corresponding sublattice and to obey the law of statistics. A corresponding pseudo unit cell is then formed by ions A, $(1-x)B$, and xC. The resulting mixed-crystal system can be thought of as a repetition of such cells. Probabilistically the pseudo unit cell may be thought of as a configurational average unit cell. A schematic representation of the pseudo unit cell for a mixed crystal in one dimension is given in Fig. 1. The fractional amount of the B and C ions located at the same lattice site is proportional to the mixing ratio in the crystal. This means that the corresponding forces involving these ions are weighted by these factors.

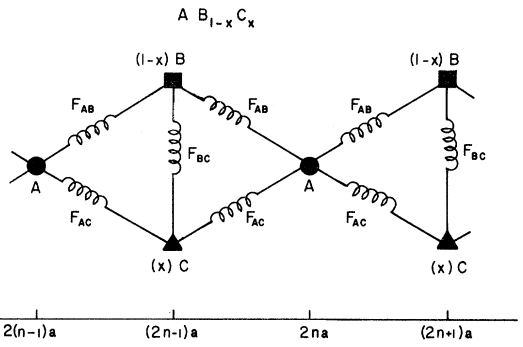

FIG. 1. Pseudo unit cell for a mixed linear diatomic chain, $AB_{1-x}C_x$ $(0 \leq x \leq 1)$.

B. Lattice dynamics

The generalized equations of motion in a mixed diatomic linear chain may be written

$$
\begin{aligned}
m_A \ddot{u}^A_{2n} &= (1-x)\sum_m (F^m_{AB}+\Phi^m_{AB})(u^B_{2n+m}-u^A_{2n}) + x\sum_m (F^m_{AC}+\Phi^m_{AC})(u^C_{2n+m}-u^A_{2n}) + \sum_l (F^l_{AA}+\Phi^l_{AA})(u^A_{2n+l}-u^A_{2n}),\\
(1-x)m_B \ddot{u}^B_{2n+1} &= (1-x)\sum_m (F^m_{AB}+\Phi^m_{AB})(u^A_{2n+1+m}-u^B_{2n+1}) + (1-x)^2\sum_l (F^l_{BB}+\Phi^l_{BB})(u^B_{2n+1+l}-u^B_{2n+1}) \\
&\quad + x(1-x)F_{BC}(u^C_{2n+1}-u^B_{2n+1}) + x(1-x)\sum (F^l_{BC}+\Phi^l_{BC})(u^C_{2n+1+l}-u^B_{2n+1}),
\end{aligned}
\tag{1}
$$

and

$$
\begin{aligned}
(x)m_C \ddot{u}^C_{2n+1} &= x\sum_m (F^m_{AC}+\Phi^m_{AC})(u^A_{2n+1+m}-u^C_{2n+1}) + x^2\sum_l (F^l_{CC}+\Phi^l_{CC})(u^C_{2n+1+l}-u^C_{2n+1}) \\
&\quad + x(1-x)F_{BC}(u^B_{2n+1}-u^C_{2n+1}) + x(1-x)\sum_l (F^l_{BC}+\Phi^l_{BC})(u^B_{2n+1+l}-u^C_{2n+1}),
\end{aligned}
$$

where $l=\pm2, \pm4, \pm6, \ldots$, and $m=\pm1, \pm3, \pm5, \ldots$, $m_{A,B,C}$ are the atomic masses, and u^{A}_{2n} and $u^{B,C}_{2n+1}$ are the atomic displacements. The subscripts represent the ion's position. $F^{j}_{KK'}$ and $\Phi^{j}_{KK'}$ are the force constants representing the jth-neighbor repulsive and the electrostatic (Coulomb) interactions, respectively, between the Kth and K'th ions. It should be pointed out that the force constant F_{BC} is an unphysical force constant inherent in the model.

The electrostatic force constants are defined as

$$\Phi^{j}_{KK'} = -\frac{d^2}{dx^2}\left(\frac{e_K e_{K'}}{x}\right)_{x=|r_j|} , \tag{2}$$

where

$$e_K = -e_{K'} = ze .$$

z is the effective ionic charge and r_j is the distance between the ions K and K'. The B and C ions are assumed to have the same effective ionic charge, therefore,

$$\Phi^{m}_{AB} = \Phi^{m}_{AC} = \Phi^{m}_{12}$$

and

$$\Phi^{l}_{AA} = \Phi^{l}_{BB} = \Phi^{l}_{CC} = \Phi^{l}_{BC} = \Phi^{l}_{11} . \tag{3}$$

Assuming a traveling wave solution of the form

$$u^{A}_{2n} = u_A e^{i(k\,2n\,a-\omega t)}$$

and

$$u^{B,C}_{2n+1} = u_{B,C}\, e^{i[k(2n+1)a-\omega t]} , \tag{4}$$

where ω is the angular frequency, k is the wave vector, and a is the lattice spacing, and Eq. (1) reduces to the following secular equation for the normal modes of vibration:

$$|\underline{D} - \omega^2 \underline{I}| = 0 . \tag{5}$$

$\underline{I}$ is the identity matrix, and the dynamical matrix $\underline{D}$ is a 3×3 symmetrical matrix. The three roots of Eq. (5) give two optic modes and one acoustic mode. In the limit of infinite dilution (as $x\to0$ and $x\to1$), two of the above solutions become the acoustic and optic modes of the host lattice, while the third mode becomes the impurity mode.

Explicit lattice-dynamical calculations were performed considering nearest-neighbor repulsive interactions and long-range Coulomb interactions. It was assumed that the force constants vary linearly with concentration from one end member to the other as

$$\frac{F_{AB}}{F_{ABO}} = \frac{F_{AC}}{F_{ACO}} = \frac{F_{BC}}{F_{BCO}} = 1-\theta x , \tag{6}$$

where the subscript O indicates the force constant appropriate for the material AB, AC, or BC.

The solution of Eq. (5) in the long-wavelength limit gives three vibrational frequencies. One of these frequencies is zero and refers to the acoustic mode of the system. The remaining two modes pertain to the optic mode of the host lattice and the impurity mode. These solutions are given as, at $x=0$,

$$\omega^2_{\mathrm{LO},AB} = (1/\mu_{AB})[\,2F_{ABO} + 4.2072(z_1^2e^2/a_1^3)]$$

and

$$\omega^2_{I,C} = (1/m_C)[\,2F_{ACO} + F_{BCO} + 3.6062(z_1^2e^2/a_1^3)] \tag{7}$$

$$= \text{Impurity mode of } C \text{ in } AB,$$

at $x=1$, we have

$$\omega^2_{\mathrm{LO},AC} = (1/\mu_{AC})[\,2F_{ACO}(1-\theta) + 4.2072(z_2^2e^2/a_2^3)]$$

and

$$\omega^2_{I,B} = (1/m_B)[(2F_{ABO} + F_{BCO})(1-\theta) + 3.6062(z_2^2e^2/a_2^3)] \tag{8}$$

$$= \text{Impurity mode of } B \text{ in } AC.$$

z_1 and a_1 refer to the AB system, z_2 and a_2 refer to the AC system, and μ_{AB} and μ_{AC} are the reduced masses. The term z^2e^2/a^3 is a force-constant-type term and is assumed to vary linearly with x as

$$z^2e^2/a^3 = F_Z = F_{ZO}(1-\theta x) . \tag{9}$$

It was assumed that $z_1 = 1.0$. This enables the complete determination of the force constant parameters F_{ABO}, F_{ACO}, F_{BCO}, F_{ZO}, and θ.

The phonon frequencies for the entire composition ranges $0 \leq x \leq 1$ can now be obtained by solving the secular equation (5) at different points in k space.

C. Frequency distribution function

The frequency distribution function as a function of the squared frequencies is defined as

$$D(\omega^2) = \frac{dM(\omega^2)}{d(\omega^2)} , \tag{10}$$

where the integrated frequency spectrum $M(\omega^2)$ is the fraction of phonon states the squares of whose frequencies are less than or equal to ω^2. This can be expressed for the mixed-crystal case as

$$M(\omega^2) = \frac{1}{N}\int_0^{\omega^2} \sum_{k,j} |\vec{e}(k|j)|^2\, \delta(y-\omega_j^2(k))\,dy , \tag{11}$$

where

$$|\vec{e}(k|j)|^2 = |\vec{u}_A(k|j)|^2 + (1-x)|\vec{u}_B(k|j)|^2 + x|\vec{u}_C(k|j)|^2 .$$

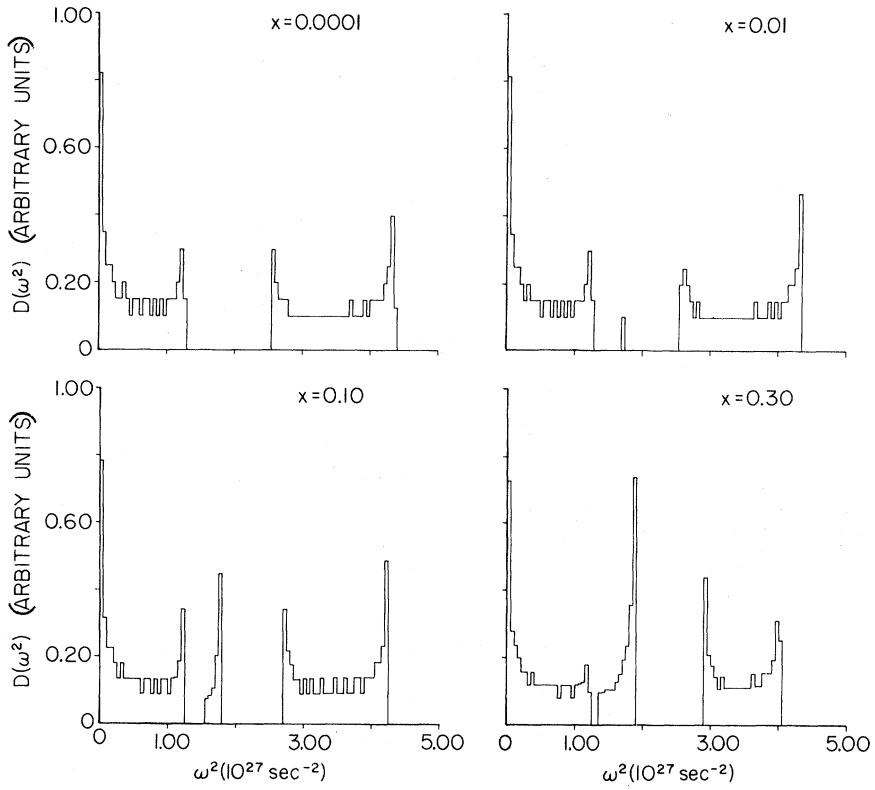

FIG. 2. Frequency distribution function for the $ZnS_{1-x}Se_x$ case at concentrations of $x=0.0001$, 0.01, 0.10, and 0.30.

$\vec{u}_A(k|j)$, $\vec{u}_B(k|j)$, and $\vec{u}_C(k|j)$ are the eigenvectors for the frequency $\omega_j(k)$, and N is the total number of phonon states.

The model parameters were determined using the value of physical observables appropriate to $ZnS_{1-x}Se_x$. This was done in order to get physically realizable values for the results. The corresponding lattice-dynamical results are in no way related to the actual results of the three-dimensional mixed crystals, which follow.

The frequency distribution function for the $ZnS_{1-x}Se_x$ case are presented in Figs. 2 and 3. At $x=0.0001$, which is a case of isolated impurities of Se in ZnS, the frequency distribution function is essentially of the perfect ZnS system. But as x is increased, the impurities begin to play an increasing role in the spectrum and consequently one notes a gradual emergence of the impurity frequency band in the gap of the optic and acoustic band. With increasing concentration, the frequency distribution in the impurity band increases while it goes on decreasing in the optic band. As x approaches unity one also notes the turning of the optic mode into the impurity mode and vice versa. And finally, at $x=0.9999$, the frequency distribution function is essentially that of the pure ZnS system.

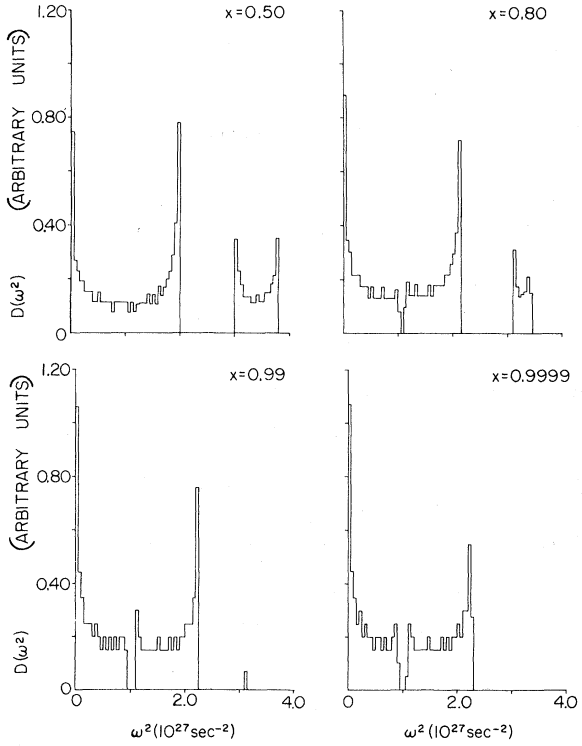

FIG. 3. Frequency distribution function for the $ZnS_{1-x}Se_x$ case at concentration of $x=0.50$, 0.80, 0.99, and 0.9999.

III. MIXED ZINC-BLENDE LATTICE

A. Lattice-dynamical model

In the three-dimensional zinc-blende lattice the A ions are located at their normal lattice site, while their nearest-neighbor site consists of a fractional amount of B and C ions proportional to the mixing ratio in the crystal. The interactions between the constituent particles in the lattice are assumed to be of the same type as described in the MRI model.[15] Basically, these interactions consist of short-range noncentral and central interactions and long-range electrostatic interactions. For near-neighbor short-range interactions, this gives rise to five repulsive force constants α_1, β_1, α_2, β_2, and α_3. The subscripts 1, 2, and 3 refer to A-B, A-C, and B-C interactions, respectively. The second-neighbor interactions are assumed to be central, giving rise to three force constants μ_1, μ_2, and μ_3. Repulsive interactions beyond second neighbors are neglected. The only parameter associated with the electrostatic interactions is the effective ionic charge parameter z.

The lattice constant a and the effective ionic charge parameter are assumed to vary linearly from one end to the other as

$$z = (1-x)z_1 + xz_2 \tag{12}$$

and

$$a = (1-x)a_1 + xa_2 ,$$

where a_1 and z_1 refer to the crystal AB, and a_2 and z_2 refer to the crystal AC. The linear variation of the lattice constants has been substantiated experimentally.[16] The force constants are also assumed to vary linearly as

$$\frac{\alpha_1}{\alpha_{10}} = \frac{\alpha_2}{\alpha_{20}} = \frac{\alpha_3}{\alpha_{30}} = \frac{\beta_1}{\beta_{10}} = \frac{\beta}{\beta_{20}} = \frac{\mu_1}{\mu_{10}} = \frac{\mu_2}{\mu_{20}} = \frac{\mu_3}{\mu_{30}} = 1 - \theta x , \tag{13}$$

where θ can be thought of as a model parameter.

The generalized equations of motion for the mixed-crystal system $AB_{1-x}C_x$ under the assumption of a traveling wave solution can be reduced to,

$$[\underline{D} - \omega^2 \underline{I}][\underline{u}] = 0 . \tag{14}$$

$\underline{I}$ is the identity matrix and $\underline{u}$ is a 1×9 column matrix. The dynamical matrix $\underline{D}$ is a 9×9 Hermitian matrix, the elements of which are of the form

$$D_{xy}(KK', \vec{k}) = [1/(m_K m_{K'})^{1/2}]\, T_{xy}(KK') . \tag{15}$$

The coupling coefficient term $T_{xy}(KK')$ is defined as

$$T_{xy}(KK') = \sum_l (\Phi^l_{KK'})_{xy}\, e^{i2\pi \vec{k}\cdot\vec{r}^{\,l}_{K'K}} , \tag{16}$$

where $K, K' = A, B, C$, and

$$(\Phi^l_{KK'})_{xy} = \frac{\partial^2 \Phi^l_{KK'}}{\partial x\, \partial y} .$$

$\vec{r}^{\,l}_{K'K}$ is the static position vector between the ions K and K', and $(\Phi^l_{KK'})_{xy}$ is the interaction potential between the Kth and K'th ions. The condition for a nontrivial solution for the displacement is

$$|\underline{D} - \omega^2 \underline{I}| = 0 . \tag{17}$$

The coupling coefficients consist of both a repulsive part, $R_{xy}(KK')$ and an electrostatic part, $C_{xy}(KK')$. Utilizing Eq. (16) along with the symmetry of the zinc-blende structure, the repulsive coupling coefficients for the first- and second-neighbor interactions are given as follows:

$$\begin{aligned}
R_{xx}(AA) &= (1-x)[4\alpha_1 + \mu_1(2 - C_{xyz})] \\
&\quad + x\{4[\alpha_2 + \mu_2(2 - C_{xyz})]\} , \\
R_{xx}(BB) &= 4[\alpha_1 + (1-x)\mu_1(2 - C_{xyz}) + x(\alpha_3 + 2\mu_3)] , \\
R_{xx}(CC) &= 4[\alpha_2 + x\mu_2(2 - C_{xyz}) + (1-x)(\alpha_3 + 2\mu_3)] , \\
R_{xx}(AB) &= \frac{(1-x)^{1/2}}{(x)^{1/2}} \frac{\alpha_1}{\alpha_2} R_{xx}(AC) \\
&= -(1-x)^{1/2}\alpha_1(a_1' + a_2' + a_3' + a_4') , \\
R_{xx}(BC) &= -4[x(1-x)]^{1/2}(\alpha_3 + \mu_3 C_{xyz}) , \\
R_{xy}(BB) &= \frac{(1-x)\mu_1}{x\mu_2} R_{xy}(CC) \\
&= \frac{(1-x)^{1/2}}{(x)^{1/2}} \frac{\mu_1}{\mu_3} R_{xy}(BC) \\
&= 4(1-x)\mu_1 \sin\pi q_x \sin\pi q_y , \\
R_{xy}(AA) &= R_{xy}(BB) + R_{xy}(CC) , \\
R_{xy}(AB) &= \frac{(1-x)^{1/2}\beta_1}{(x)^{1/2}\beta_2} R_{xy}(AC) \\
&= -(1-x)^{1/2}\beta_1(a_1' + a_2' - a_3' - a_4'), \\
R_{xz}(AB) &= \frac{(1-x)^{1/2}\beta_1}{(x)^{1/2}\beta_2} R_{xz}(AC) \\
&= (1-x)^{1/2}\beta_1(a_1' - a_2' + a_3' - a_4') , \\
R_{yz}(AB) &= \frac{(1-x)^{1/2}\beta_1}{(x)^{1/2}\beta_2} R_{yz}(AC) \\
&= -(1-x)^{1/2}\beta_1(a_1' - a_2' - a_3' - a_4') ,
\end{aligned} \tag{18}$$

where

TABLE I. Physical observables for zinc-blende crystals; ω in cm^{-1}; C_{ij} in 10^{11} dyn/cm^2.

	C_{11}	C_{12}	C_{44}	Ref.	ω_{LO}	ω_{TO}	ω_I	Ref.
ZnS	10.46	6.53	4.613	20	350	270	220 [a]	19
ZnSe	8.59	5.06	4.06	20	252	206	297 [b]	19
GaP	14.11	6.187	7.043	22	406	366	270 [c]	9, 21
GaAs	11.877	5.372	5.944	23	295.5	268	355 [b]	9, 20

[a] Extrapolated gap mode.
[b] Local mode.
[c] Gap mode.

$$C_{xyz} = \cos\pi q_x \cos\pi q_y + \cos\pi q_z \cos\pi q_x \ ,$$
$$a_1' = e^{i\pi(q_x+q_y+q_z)/2} \ ,$$
$$a_2' = e^{i\pi(q_z-q_x-q_y)/2} \ , \qquad (19)$$
$$a_3' = e^{i\pi(q_y-q_x-q_z)/2} \ ,$$
$$a_4' = e^{i\pi(q_x-q_y-q_z)/2} \ ,$$

and

$$\vec{q} = (a/2\pi)\vec{k} \ .$$

A cyclic permutation of the coordinates (x, y, z) along with the use of the Hermitian property of the coupling coefficients enables one to generate the remaining repulsive coupling coefficients. The electrostatic part of the coupling coefficient is due to Coulomb interactions between ions of appropriate effective ionic charge. General expressions for the Coulomb coupling coefficients of the perfect crystals have been given by Woods *et al.*[17] Extension of this work to the mixed zinc-blende crystals is straightforward.[18] For the special case of $\vec{k}=0$ tending to zero from the x direction, the only nonzero Coulomb coupling coefficients for the mixed-crystal case are

$$C_{xx}(AA) = -2C_{yy}(AA) = -2C_{zz}(AA) = C_z \ ,$$
$$C_{xx}(BB) = -2C_{yy}(BB) = -2C_{zz}(BB) = (1-x)C_z \ ,$$
$$C_{xx}(CC) = -2C_{yy}(CC) = -2C_{zz}(CC) = xC_z \ , \qquad (20)$$
$$C_{xx}(AB) = -2C_{yy}(AB) = -2C_{zz}(AB) = -(1-x)^{1/2}C_z \ ,$$
$$C_{xx}(AC) = -2C_{yy}(AC) = -2C_{zz}(AC) = -(x)^{1/2}C_z \ ,$$

and

$$C_{xx}(BC) = -2C_{yy}(BC) = -2C_{zz}(BC) = [x(1-x)]^{1/2}C_z$$

where

$$C_z = 8\pi z^2 e^2/3v_a$$

and

$$v_a = \tfrac{1}{4}a^3 \ .$$

B. Model parameters

The model parameters contained in the coupling coefficients are determined by relating them to known elastic constants and the long-wavelength vibrational modes of the system AB as $x \to 0$ and the system AC as $x \to 1$. The relations between the elastic constants and the model parameters can be expressed at $x=0$ as

$$C_{11,1} = \frac{1}{2r_1}(\alpha_{10}+8\mu_{10}) + 0.1255\frac{z_1^2e^2}{2r_1^4} \ ,$$
$$C_{12,1} = \frac{1}{2r_1}(2\beta_{10}-\alpha_{10}+4\mu_{10}) - 1.324\frac{z_1^2e^2}{2r_1^4} \ , \qquad (21)$$

and

$$C_{44,1} = \frac{1}{2r_1}(\alpha_{10}+4\mu_{10}) - 0.063\frac{z_1^2e^2}{2r_1^4} - \frac{[2.519(z_1^2e^2/2r_1^5) - (\beta_{10}/r_1^2)]^2}{2\alpha_{10}/r_1^3 - \pi z_1^2e^2/3r_1^6} \ ,$$

and at $x=1$ as,

$$C_{11,2} = \frac{1}{2r_2}(\alpha_{20}+8\mu_{20})(1-\theta) + 0.1255\frac{z_2^2e^2}{2r_2^4} \ ,$$
$$C_{12,2} = \frac{1}{2r_2}(2\beta_{10}-\alpha_{20}+4\mu_{20})(1-\theta) - 1.324\frac{z_2^2e^2}{2r_2^4} \ ,$$

and

$$C_{44,2} = \frac{1}{2r_2}(\alpha_{20}+4\mu_{20})(1-\theta) - 0.063\frac{z_2^2e^2}{2r_2^4} - \frac{[2.519(z_2^2e^2/2r_2^5) - \beta_{20}(1-\theta)/r_2^2]^2}{2\alpha_{20}(1-\theta)/r_2^3 - \pi z^2e^2/3r_2^6} \ , \qquad (22)$$

where r_1, $r_2 = \frac{1}{2}(a_1, a_2)$. The second subscripts 1 and 2, in the elastic constants refer to the systems AB and AC, respectively. The long-wavelength vibrational mode frequencies can be related to the force-constant parameters by evaluating the secular equations for the eigenfrequencies of vibration at $\vec{k}=0$.

The following expressions may be shown to result, first, at $x=0$,

$$\omega^2 = 0 = \omega^2_{\mathrm{LA},\,AB} = \omega^2_{\mathrm{TA},\,AB}\ , \tag{23}$$

$$\omega^2 = (1/\mu_{AB})[\ \alpha_{10} + \tfrac{8}{3}\pi z_1^2 e^2/v_{a_1}\ ] = \omega^2_{\mathrm{LO},\,AB}\ , \tag{24}$$

$$\omega^2 = (1/\mu_{AB})[\ \alpha_{10} - \tfrac{4}{3}\pi z_1^2 e^2/v_{a_1}\ ] = \omega^2_{\mathrm{TO},\,AB}\ , \tag{25}$$

and

$$\omega^2 = (1/m_C)(4\alpha_{20} + \alpha'_{30}) = \omega^2_{I,\,C}$$
$$= \text{impurity mode of } C \text{ in } AB\ , \tag{26}$$

and then at $x=1$,

$$\omega^2 = 0 = \omega^2_{\mathrm{LA},\,AC} = \omega^2_{\mathrm{TA},\,AC}\ , \tag{27}$$

$$\omega^2 = (1/\mu_{AC})[\ 4\alpha_{20}(1-\theta) + \tfrac{8}{3}\pi(z_2^2 e^2/v_{a_2})]$$
$$= \omega^2_{\mathrm{LO},\,AC}\ , \tag{28}$$

$$\omega^2 = (1/\mu_{AC})[\ 4\alpha_{20}(1-\theta) - \tfrac{4}{3}\pi(z_2^2 e^2/v_{a_2})]$$
$$= \omega^2_{\mathrm{TO},\,AC}\ , \tag{29}$$

and

$$\omega^2 = (1/m_B)(4\alpha_{10} + \alpha'_{30})(1-\theta) = \omega^2_{I,\,B}$$
$$= \text{impurity mode of } B \text{ in } AC\ , \tag{30}$$

where

$$\alpha'_{30} = 4(\alpha_{30} + 2\mu_{30})$$

and (31)

$$1/\mu_{AB,\,C} = 1/m_A + 1/m_{B,\,C}\ .$$

All the transverse frequencies above are doubly degenerate and the degeneracy of the impurity frequencies is threefold. The zero-frequency solution for the acoustic mode confirms that the model is consistent with the continuum case at long wavelengths. For a system exhibiting two-mode behavior, the impurity modes in Eqs. (26) and (30) are the gap and local modes. For one-mode systems, the resonant modes are thought of as being the impurity modes. In the case where the systems exhibit mixed mode behavior, a combination of resonant mode and gap or local modes may be appropriate.

Since there is an imbalance between the number of equations and unknown parameters, some of these equations were solved in the least-square sense. Equations (24)–(26) and (28)–(30) were solved simultaneously for α_{10}, α_{20}, α_{30}, z_1, and z_2. The remaining model parameters were obtained by solving Eqs. (21) and (22) by a least-squares method. The expressions for the least-square error were formed as follows:

$$\epsilon_1^2 = (C_{11,1} - C'_{11,1})^2 + (C_{12,1} - C'_{12,1})^2 + (C_{44,1} - C'_{44,1})^2$$

and (32)

$$\epsilon_2^2 = (C_{11,2} - C'_{11,2})^2 + (C_{12,2} - C'_{12,2})^2 + (C_{44,2} - C'_{44,2})^2\ .$$

The primed elastic constants are the expressions given by Eqs. (21) and (22) with the α_{10}, z_1, α_{20}, and z_2 paramters obtained from Eqs. (24)–(26) and (28)–(30). The unknown parameters β_{10}, μ_{10}, β_{20}, and μ_{20} were then obtained by simultaneously solving

$$\frac{\partial\epsilon_1^2}{\partial\mu_{10}} = 0,\quad \frac{\partial\epsilon_1^2}{\partial\beta_{10}} = 0\ ,$$

and (33)

$$\frac{\partial\epsilon_2^2}{\partial\mu_{20}} = 0,\quad \frac{\partial\epsilon_2^2}{\partial\beta_{20}} = 0\ .$$

Since the value of the second-neighbor repulsive force constant for B-C interaction might be expected tc be somewhere between the values of a second-neighbor B-B- and C-C-type force constants, it was assumed that

$$\mu_{30} = (\mu_{10}\mu_{20})^{1/2}\ . \tag{34}$$

This makes the determination of α_{30} from Eq. (31) possible.

C. Phonon dispersion

The phonon dispersion curves for the mixed zinc-blende crystals were obtained by solving the secular equation as a function of wave vector and concentration. Table I lists all the physical observables used as input parameters and the resulting model parameters are summarized in Table II. Figures 4 and 5 present explicit phonon dispersion curves for $ZnS_{1-x}Se_x$ and $GaP_{1-x}As_x$

TABLE II. Force-constant parameters for mixed zinc-blende crystals; α, β, and μ, in 10^5 dyn/cm.

$AB_{1-x}C_x$	α_{10}	β_{10}	μ_{10}	α_{20}	β_{20}	μ_{20}	α_{30}	μ_{30}	Z_1	Z_2	θ
$ZnS_{1-x}Se_x$	0.2838	0.3187	0.0337	0.3661	0.3311	0.3406	0.1699	0.0339	0.9309	0.8326	0.1999
$GaP_{1-x}As_x$	0.4563	0.3697	0.0364	0.5249	0.4261	0.0392	0.2051	0.0378	0.7365	0.7137	0.2188

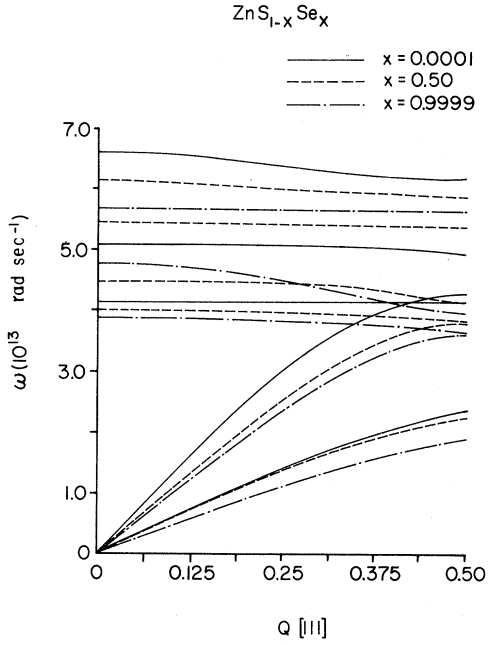

FIG. 4. Phonon dispersion for $ZnS_{1-x}Se_x$ in the [111] direction. Solid line, $x=0.0001$; dotted line, $x=0.50$; dot-dash line, $x=0.9999$.

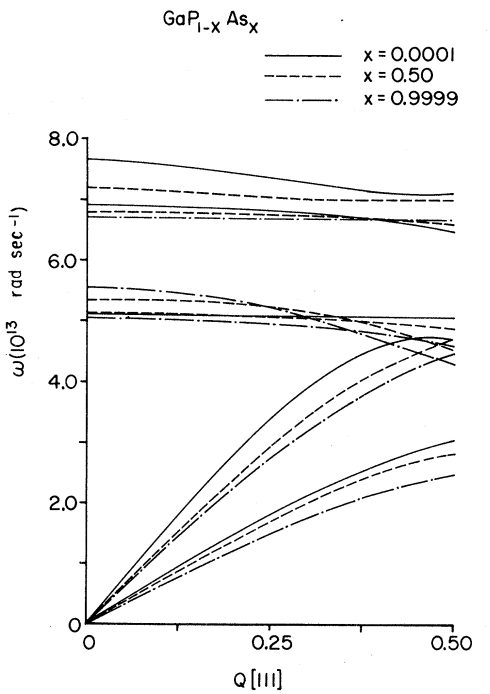

FIG. 5. Phonon dispersion for $GaP_{1-x}As_x$ in the [111] direction. Solid line, $x=0.0001$; dotted line, $x=0.50$; dot-dash line, $x=0.9999$.

as a function of wave vector in the [111] direction for various values of concentration. For the $Zn_{1-x}Se_x$ systems, the impurity mode at $x\to 0$, was taken to be the extrapolated gap mode.[19] The present calculations predict the impurity mode of Se in ZnS as $x\to 0.0$ to be a resonant mode; see Fig. 4. Thus $ZnS_{1-x}Se_x$ does not exhibit the true two-mode behavior and further classification of this system is necessary. The $GaP_{1-x}As_x$ system exhibits two-mode behavior and, indeed, one observes the gap mode at $x=0.0001$ and the local mode at $x=0.9999$.

In general, one observes nine distinct branches of phonon dispersion for an arbitrary direction in $\vec{k}$ space for the mixed zinc-blende crystals. Three of these branches refer to the acoustic mode of the system. Of the remaining branches, three are the optical mode frequencies of the host lattice and the other three are the impurity mode frequencies of the system. In the limits of infinite dilution as $x\to 0.0$ and $x\to 1.0$, the impurity modes are triply degenerate throughout the $\vec{k}$ space. The nondispersive behavior of the impurity modes for infinite dilution is quite evident in Figs. 4 and 5. As the concentration departs from these limits of infinite dilution, the impurity mode starts to show dispersion, while the optic mode becomes less dispersive. The long-wavelength optical phonons in $ZnS_{1-x}Se_x$ and $GaP_{1-x}As_x$ mixed systems are presented as a function of concentration in Figs. 6 and 7. These predictions are in good agreement with the experiments[7,8,19] and the modified random-element-isodisplacement (REI) model calculations.[9] In Sec. III, it has also been shown that the isolated impurities as $x\to 0.0$ and $x\to 1.0$ give rise to triply degenerate localized vibrational modes. When the impurity concentration is increased, these threefold degenerate localized modes split into twofold degenenerate transverse modes and a nondegenerate longitudinal mode. This splitting behavior is in agreement with a previous prediction.[24]

D. Frequency distribution

Utilizing Eq. (11) the frequency distribution function is calculated for a mesh of 4096 points in the first Brillouin zone. Owing to the symmetry properties of the Brillouin zone for the zinc-blende structure one needs to consider the determination of the eigenfrequencies only at the nonequivalent points in the $\vec{k}$ space defined as

$$\vec{k}=(\pi/8a)(q_x,q_y,q_z)\ ,$$

where

$$16\geq q_x\geq q_y\geq q_z\geq 0 \tag{35}$$

and

$$q_x+q_y+q_z\geq 24\ .$$

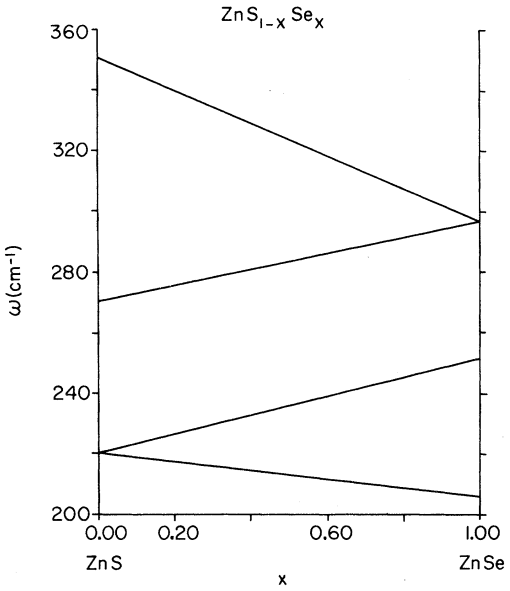

FIG. 6. Long-wavelength optical phonons in $ZnS_{1-x}Se_x$ as a function of concentration x.

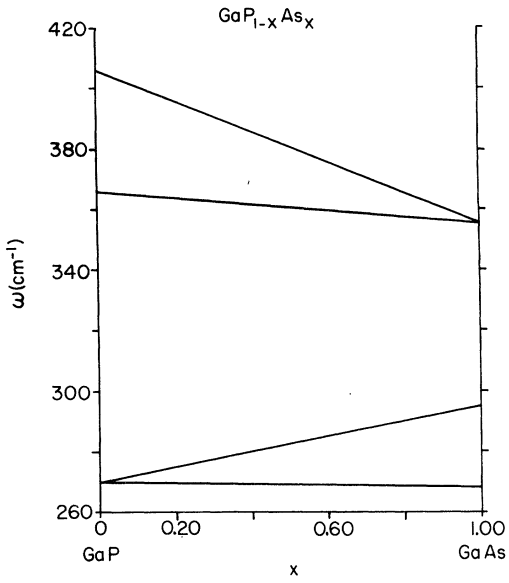

FIG. 7. Long-wavelength optical phonons in $GaP_{1-x}As_x$ as a function of concentration x.

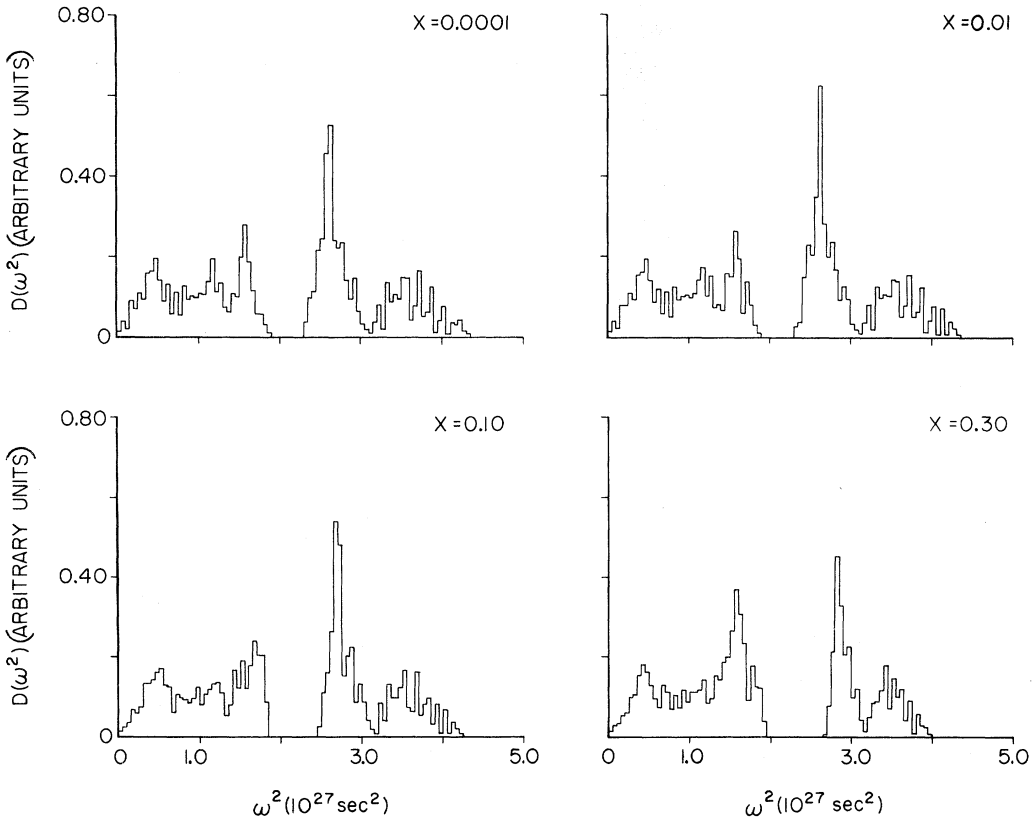

FIG. 8. Frequency distribution function for $ZnS_{1-x}Se_x$ for various values of concentration, $x_1 = 0.0001$, 0.010, 0.10, and 0.30.

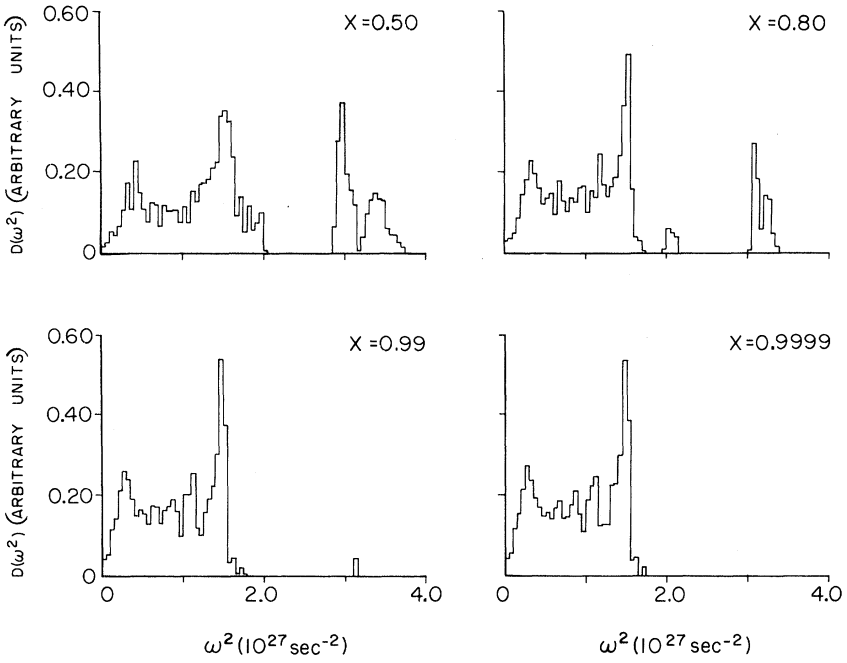

FIG. 9. Frequency distribution function for $ZnS_{1-x}Se_x$ for various values of concentration x =0.50, 0.80, 0.99, and 0.9999.

This particular mesh of $\vec{k}$ points gives a total of 24 567 frequencies from which a histogram of the distribution function is obtained.

The frequency distribution functions for $ZnS_{1-x}Se_x$ and $GaP_{1-x}As_x$ systems have been calculated for various values of x and are presented in Figs. 8–11. In the case of $ZnS_{1-x}Se_x$, one does not observe an impurity mode emerging in the gap of the distribution function when the concentration is increased from 0.0001. What

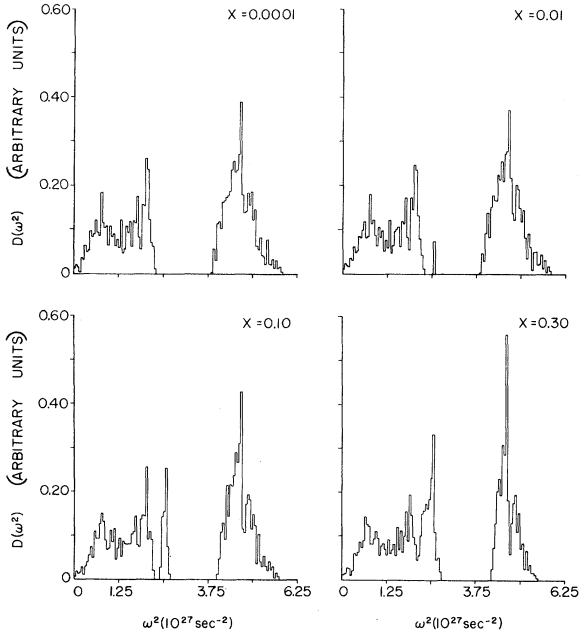

FIG. 10. Frequency distribution function for $GaP_{1-x}As_x$ for various values of concentration x =0.0001, 0.010, 0.10, and 0.30.

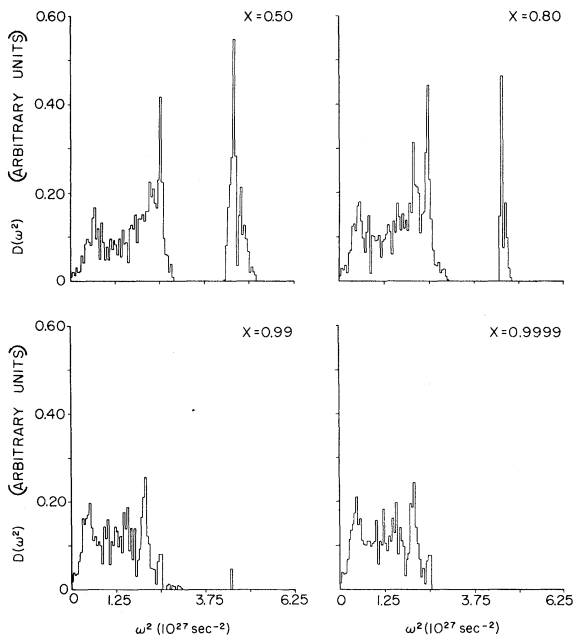

FIG. 11. Frequency distribution function for $GaP_{1-x}As_x$ for various values of concentration x =0.50, 0.80, 0.99, and 0.9999.

one notes is a peak rising near the top of the acoustic band. This suggests that the impurity mode in $ZnS_{1-x}Se_x$ as $x \to 0.0$ is a resonant mode. This is substantiated by the fact that Chang and Mitra[19] extrapolated their long-wavelength results for $ZnS_{1-x}Se_x$ to $x \to 0.0$, but they could only measure the gap-mode behavior to a concentration of $x \approx 0.2$. The emergence of the gap and local modes in $GaP_{1-x}As_x$ systems, is self-explanatory.

IV. DISCUSSION

Since no neutron-scattering data exist for the phonon dispersion in mixed zinc-blende crystals no direct comparison can be made with experiment. The only known neutron data on dispersion curves in mixed crystals were obtained for $K_xRb_{1-x}Br$.[25] It was observed in this work that the transverse-acoustic and transverse-optic modes in the [111] direction decreased with an increasing concentration of the Rb ion. Our results on $GaP_{1-x}As_x$ and $ZnS_{1-x}Se_x$ in the [111] direction show a similar type of trend as the concentration of the As and Se ions, respectively, is increased.

The present model is proposed for the entire composition range $0 \leq x \leq 1$, therefore it reduces to the vibrational spectrum and predicts impurity frequencies for the crystal AB with isolated impurities C, in the limit of x approaching zero and likewise also reduces to a corresponding prediction for the crystal AC with isolated impurities B, in the limit of x approaching unity. Since this theory is also proposed to predict the phonon dispersion behavior throughout the Brillouin zone, it also predicts the $\vec{k} = 0$ phonons of the mixed crystals at all values of concentration. The present model essentially is an interpolation scheme between two perfect crystals. It is, however, capable of predicting impurity mode behavior. These modes have flat dispersion at low concentration and then become increasingly dependent on k as concentration increases. This is the behavior one would expect in k-conserving neutron-scattering experiments.

Since a more physically realizable model capable of yielding phonon dispersion and the frequency distribution has yet to be applied in detail for three-dimensional lattices, the present model might serve as a useful tool in analyzing experimental results on mixed-crystal systems.

In order to further test the present approach more neutron-scattering data on mixed crystals are needed.

ACKNOWLEDGMENT

The authors wish to extend their thanks to Dr. Kasinath V. Namjoshi for helpful discussions.

---

*Present address: Dept. of Electrical Engineering, McGill University, Montreal, Canada.

[1]F. Krueger, O. Reinkober, and E. Koch-holn, Ann. Phys. (Leipz.) 85, 110 (1928).
[2]I. M. Lifschitz, J. Phys. USSR 7, 215 (1943); 7, 249 (1943); 8, 89 (1944).
[3]I. Prigogine, R. Birgen, and J. Jeener, Physica (Utr.) 20, 383 (1954); 20, 516 (1954).
[4]I. M. Lifschitz and G. I. Stephanova, Sov. Phys.-JETP 3, 656 (1956).
[5]F. Matossi, J. Chem. Phys. 19, 161 (1951).
[6]P. Dean, Proc. Phys. Soc. Lond. 73, 413 (1959); Proc. R. Soc. A 254, 507 (1960); 260, 263 (1961).
[7]H. W. Verleur and A. S. Barker, Phys. Rev. 149, 715 (1966); 155, 750 (1967).
[8]Y. S. Chen, W. Shockley, and G. L. Pearson, Phys. Rev. 151, 648 (1966).
[9]I. F. Chang and S. S. Mitra, Phys. Rev. 172, 924 (1968).
[10]I. F. Chang and S. S. Mitra, Adv. Phys. 20, 359 (1971).
[11]A. P. G. Kutty, Solid State Commun. 14, 213 (1974).
[12]D. W. Taylor, Solid State Commun. 13, 117 (1973).
[13]P. N. Sen and W. M. Hartmann, Phys. Rev. B 9, 367 (1974).
[14]T. Kaplan and M. Mostoller, Phys. Rev. B 9, 353 (1974); 9, 1783 (1974).
[15]J. F. Vetelino and S. S. Mitra, Phys. Rev. 178, 1349 (1969).
[16]L. Vegard, Skr. Nor. Vidensk. Akad. Oslo 1 2, 83 (1947); Chem. Abstr. 43, 4073L (1949).
[17]A. D. B. Woods, W. Cochran, and B. N. Brockhouse, Phys. Rev. 119, 980 (1960).
[18]S. C. Varshney, M.S. thesis (University of Maine, 1974) (unpublished).
[19]O. Brafman, I. F. Chang, G. Lengyel, S. S. Mitra, and E. Carnall, Phys. Rev. Lett. 19, 1120 (1967); in *Proceedings of the International Conference on Localized Excitations in Solids*, edited by R. F. Wallis (Plenum, New York, 1968), p. 602.
[20]L. H. Skolnik, W. G. Spitzer, A. Kahan, and R. G. Hunsperger, J. Appl. Phys. 44, 5223 (1971).
[21]A. S. Barker, Jr., Phys. Rev. 165, 917 (1968).
[22]D. Berlincourt, H. Jaffe, and L. R. Shiozawa, Phys. Rev. 129, 1009 (1963).
[23]H. J. McSkimin, A. Jayaraman, and P. Andreatch, Jr., J. Appl. Phys. 38, 2362 (1967).
[24]A. A. Maradudin and J. Oitma, Solid State Commun. 7, 1143 (1969).
[25]S. Rolandson and G. Raunio, J. Phys. C 4, 958 (1971).